



HAL
open science

Hexanitrate complexes and hybrid double perovskites of Am^{3+} and Cm^{3+}

Michael Tarlton, Suntharalingam Skanthakumar, Valérie Vallet, Richard E. Wilson

► **To cite this version:**

Michael Tarlton, Suntharalingam Skanthakumar, Valérie Vallet, Richard E. Wilson. Hexanitrate complexes and hybrid double perovskites of Am^{3+} and Cm^{3+} . *Chemical Communications*, 2022, 58 (85), pp.11997-12000. 10.1039/D2CC05162A . hal-03868941

HAL Id: hal-03868941

<https://hal.science/hal-03868941>

Submitted on 24 Nov 2022

HAL is a multi-disciplinary open access archive for the deposit and dissemination of scientific research documents, whether they are published or not. The documents may come from teaching and research institutions in France or abroad, or from public or private research centers.

L'archive ouverte pluridisciplinaire **HAL**, est destinée au dépôt et à la diffusion de documents scientifiques de niveau recherche, publiés ou non, émanant des établissements d'enseignement et de recherche français ou étrangers, des laboratoires publics ou privés.

Cite this: DOI: 00.0000/xxxxxxxxxx

Hexanitrate complexes and hybrid double perovskites of Am^{3+} and $\text{Cm}^{3+\dagger\ddagger}$ Michael L. Tarlton,^{aa} Suntharalingam Skanthakumar,^a Valérie Vallet,^{b*} and Richard E. Wilson^{a*}

Received Date

Accepted Date

DOI: 00.0000/xxxxxxxxxx

The synthesis and structures of the homoleptic hexanitrate complexes of Am(III) and Cm(III), $[(\text{CH}_3)_4\text{N}]_2\text{KAn}(\text{NO}_3)_6$ are reported. These compounds form a double perovskite structure type, $\text{A}_2\text{B}'\text{BX}_6$, crystallizing in the cubic space group $\text{Fm}\bar{3}\text{m}$. Their electronic properties, as calculated using the Quantum Theory of Atoms in Molecules, are reported and compared to their lanthanide homologues Eu(III) and Gd(III).

Synthetic and structural studies of the *f*-elements underpin efforts at resolving fundamental questions regarding the description of *f*-element electronic structure and bonding.^{1–6} The study of periodic series of *f*-element molecules, materials, and their chemical behavior has been particularly useful in this regard by identifying and exploring trends within their chemical and physical properties.⁷ The foundational paper by Seaborg explored the chemistries of trivalent lanthanide and actinide chloride complexes.⁸ The observed differences between the *5f* and *4f* ion behavior was hypothesized to occur in part due to greater *5f* orbital participation in the metal-ligand interactions of the actinides versus the lanthanides inspiring comparative studies of trivalent actinide and lanthanide ions in a variety of chemical systems in

both solution and the solid-state.^{7,9,10} Studies of transuranium molecules and materials extends all the way to Es (*Z*=99) and has demonstrated a number of unexpected observations of the chemical and physical properties of these elements that departs from the periodic trends.^{2,3,10,11}

We have focused on the synthesis of periodic series of *f*-element molecules and materials that include mineral acid anions, e.g. SO_4^{2-} ^{12,13}, Cl^- ^{14,15}, and NO_3^- ¹⁶, that underpin much of the aqueous and economically important separations chemistry of lanthanides and actinides. We studied of a complete series of *f*-element NCS^- complexes of the trivalent actinides and lanthanides that enabled their spectroscopic study and the investigation of the metal-NCS interaction among these *f*-ions.¹⁷ Here we report the synthesis and structures of Am and Cm hexanitrate salts, $[(\text{CH}_3)_4\text{N}]_2\text{KAn}(\text{NO}_3)_6$, from aqueous solution that crystallize in the cubic space group $\text{Fm}\bar{3}\text{m}$, exhibiting the double perovskite, $\text{A}_2\text{B}'\text{BX}_6$, structure type. These two transuranium compounds are the first compounds to demonstrate hexanitrate and homoleptic nitrate coordination of the trivalent actinides, and the first structural report of any Cm nitrate to be isolated in the solid state.^{18,19} They also represent the first reports of transuranium element hybrid double perovskites that incorporate an organic cation on the A-site, expanding upon the chloride containing double perovskite phases of the trivalent lanthanide and actinide elpasolites.^{20–22}

The stoichiometric combination of $(\text{CH}_3)_4\text{N}\cdot\text{NO}_3$, KNO_3 , and either Am or Cm in 4 M HNO_3 in a 2:1:1 ratio results in the deposition of single crystals of $[(\text{CH}_3)_4\text{N}]_2\text{KAn}(\text{NO}_3)_6$ where (An: Am, Cm), after evaporation at room temperature or by gentle heating on a hotplate (Figure S1 and S2 in the ESI †). Single crystal X-ray diffraction measurements of the crystals were conducted at room temperature in the cubic space group $\text{Fm}\bar{3}\text{m}$, Table 1. The measured lattice constants and additional metrical information resulting from the crystallographic refinements are provided

^a Chemical Sciences and Engineering Division, Argonne National Laboratory, 9700 S. Cass Avenue, Lemont, IL, USA. E-mail: rewilson@anl.gov

^b Univ. Lille, CNRS, UMR 8523 – PhLAM – Physique des Lasers Atomes et Molécules, F-59000 Lille, France. E-mail: valerie.vallet@univ-lille.fr

† Electronic Supplementary Information (ESI) available: Details of the synthetic procedures, X-ray crystallography, and density functional theory calculations. See DOI: 00.0000/00000000.

‡ This work was conducted at ANL, operated by UChicago Argonne LLC for the United States Department of Energy (U.S. DOE), and supported by the U.S. DOE Office of Science, Office of Basic Energy Sciences, Chemical Sciences Geological and Biosciences Division, Heavy Element Chemistry program under Contract DE-AC02-06CH11357. VV acknowledges support by the French government through the Program “Investissement d’avenir” (Grants LABEX CaPPA/ANR-11-LABX-0005-01 and I-SITE ULNE/ANR16-IDEX-0004 ULNE), as well as by the Ministry of Higher Education and Research, Hauts de France council and European Regional Development Fund (ERDF) through the Contrat de Projets État Région (CPER CLIMIBIO). Furthermore, this work was granted access to the HPC resources of CINES/IDRIS/TGCC under the allocation 2021–2022 (A0110801859) made by GENCI.

in Table 1 and Table 2.[§]

Table 1 Results of the crystallographic refinements for the single crystal X-ray diffraction data collected for $((\text{CH}_3)_4\text{N})_2\text{KAn}(\text{NO}_3)_6$

	Am	Cm
F.W. ($\text{g}\cdot\text{mol}^{-1}$)	802.45	807.45
color	pink	colorless
Temperature (K)	298(2)	300(2)
Space Group	$Fm\bar{3}m$	$Fm\bar{3}m$
$a = b = c$ (\AA)	13.7426(11)	13.7469(11)
$\alpha = \beta = \gamma$ ($^\circ$)	90.00	90.00
Volume (\AA^3)	2595.4(6)	2597.9(6)
Z	4	4
ρ calc. ($\text{g}\cdot\text{cm}^{-3}$)	2.054	2.064
μ (mm^{-1})	3.205	3.387
λ MoK α (\AA)	0.71073	0.71073
Final R indices (all data)	$R_1 = 0.0134$ $wR^2 = 0.0314$	$R_1 = 0.0103$ $wR^2 = 0.0236$
GoF	1.093	1.018
largest peak/hole ($e/\text{\AA}^3$)	0.642/-0.227	1.265/-0.345

Table 2 Relevant bond distances as determined from the X-ray diffraction refinements for $((\text{CH}_3)_4\text{N})_2\text{KAn}(\text{NO}_3)_6$

	Am	Cm
$d(\text{An}-\text{O}_2\text{NO})$ (\AA)	2.602(3)	2.594(3)
$d(\text{K}-\text{ONO}_2)$ (\AA)	2.652(5)	2.660(5)
$d(\text{N}-\text{O})$ (\AA) NO_3^-	1.254(4), 1.267(8)	1.253(4), 1.259(8)
$d(\text{N}-\text{C})$ (\AA) $(\text{CH}_3)_4\text{N}^+$	1.466(9)	1.459(9)

The crystals are composed of $((\text{CH}_3)_4\text{N})_2\text{KAn}(\text{NO}_3)_6$ where (An: Am, Cm). This material contains twelve-coordinate hexanitrate polyhedra forming the $\text{An}(\text{NO}_3)_6$ moiety that corner share through the distal oxygen atoms of the nitrate groups to form a $\text{K}(\text{ONO}_2)_6$ octahedron. The $(\text{CH}_3)_4\text{N}^+$ occupies the voids formed by the $\text{An}(\text{NO}_3)_6$ and $(\text{CH}_3)_4\text{N}^+$ framework, Figure 1.

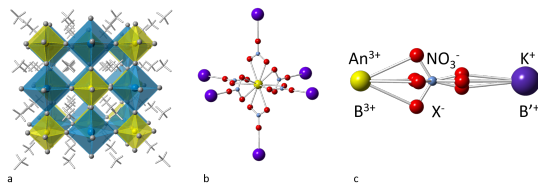


Fig. 1 Panel a., shows the face centered cubic packing. For clarity the nitrate ions have been rendered as gray spheres at the vertices of the polyhedra. The $\text{An}(\text{NO}_3)_6$ polyhedra are rendered in yellow, and the $\text{K}(\text{ONO}_2)_6$ are in teal. Panel b. presents the hexanitrate anion of the Am and Cm complexes highlighting the twelve coordinate actinide ion in yellow, and the coordination of the potassium ions, purple, by the distal oxygen atoms. In c., the crystallographic disorder of the nitrate anions is displayed with the oxygen atoms disordered about the four-fold symmetry axis.

The six nitrate groups coordinate bidentate to the Am and Cm ions located on the crystallographic origin, Wyckoff site 4a.

The $\text{Am}-\text{O}_2\text{NO}$ and $\text{Cm}-\text{O}_2\text{NO}$ bond distances are 2.602(3) \AA and 2.594(3) \AA , respectively, and reflect a slight contraction in the bond distance from Am to Cm. These bond distances are consistent with those reported for homoleptic nitrate complexes of the lanthanides such as in the molecular complexes $((\text{CH}_3)_4\text{N})_3\text{La}(\text{NO}_3)_6(\text{CH}_3\text{OH})$, 2.612-2.677 \AA , and $((\text{CH}_3)_4\text{N})_3\text{Nd}(\text{NO}_3)_6$, 2.588-2.6165 \AA .^{23,24} No prior reports of homoleptic nitrate complexes of the trivalent $5f$ ions are available. The refinements of the nitrate anions reflect occupational disorder arising from a crystallographic four-fold axis necessitating the refinement of the nitrate oxygen atoms coordinated to the actinide ion as only partially occupied (1/2). The nitrogen atom, Wyckoff 24e, of the nitrate group is crystallographically ordered. The distal oxygen atom of the nitrate groups was originally located on a special position, Wyckoff 24e, in the direct methods structure solution but in the course of the refinement the observation of larger than expected atomic displacement parameters led us to displace the oxygen atom slightly out of its collinear position with the An(III), nitrogen, and potassium atoms, Wyckoff 96j, and refining the occupancy to 0.5 reflecting the four-fold symmetry about this axis. Despite the occupational disorder associated with the nitrate anions, the N-O bond distances refine to a range of values spanning 1.253(4) to 1.267(8) \AA , with the longer bond distances associated with N-O bond bonding with the K^+ site. For reference, the N-O bond distances observed for the NO_3^- anion in KNO_3 are 1.273 \AA .²⁵

The $\text{An}(\text{NO}_3)_6$ polyhedron corner shares at the distal oxygen atoms of the NO_3^- with the potassium site forming a $\text{K}(\text{ONO}_2)_6$ octahedron. The $\text{K}-\text{ONO}_2$ bond distances from the refinements are 2.652(5) and 2.660(5) \AA , in the Am and Cm crystals respectively. The potassium ion is located on the Wyckoff 4b site and the alternating, corner-sharing polyhedra, join to form the face centered cubic lattice. The $(\text{CH}_3)_4\text{N}^+$ ions are located on the tetrahedral site, Wyckoff 8c. Disorder was noted in the terminal methyl groups and treated by refining the carbon atoms associated with them to 1/3 occupied. Provided the disorder of the organic cations, no attempt was made to model the hydrogen atom positions in the refinements.

The chemical composition and structure of these nitrate compounds results in the formation of a hybrid double perovskite structure, $\text{A}_2\text{B}'\text{BX}_6$, where the A-site is the organic cation tetramethylammonium, the potassium is on the B'-site, the Am and Cm on the B-site, and nitrate is X. This is the first report of a hybrid double perovskite of the actinide elements and expands on the halide double perovskite phases, elpasolites, of the transuranium elements synthesized by Bagnall²² and Morss²⁰ to now include hybrid perovskite phases.²⁶ Bagnall originally synthesized the chloride containing double perovskite $\text{Cs}_2\text{NaAmCl}_6$ from an aqueous solutions saturated with HCl and a similar approach was taken by Morss and Fuger in the synthesis of $\text{Cs}_2\text{NaBkCl}_6$. The elpasolites crystallize in cubic symmetry, a property which has been exploited to study the spectroscopic and magnetic properties of $5f$ -ions.^{27,28}

The inclusion of polyatomic anions on the X-site in perovskites has been of recent synthetic interest including HCO_2^- , CN^- , BH_4^- , NO_3^- , and H_2PO_2^- .²⁹⁻³¹ Trivalent lanthanide nitrate con-

[§] Summaries of the crystallographic refinements are provided as CIFs including the structure factors and have been deposited with the Cambridge Crystallographic Data Center, CCDC, retrievable under accession codes 2168158 (Am) and 2168159 (Cm).

taining double perovskites have been synthesized as both layered and three dimensional structures and their phase behavior and ferroelectric properties have been studied.^{32–34} The reported nitrate containing double perovskites are all based on hexanitrate complexes of the lanthanides like those reported here. Twelve coordinate hexanitrate complexes are most frequently encountered in tetravalent lanthanide and actinide molecular complexes like $(\text{NH}_4)_2\text{Ce}(\text{NO}_3)_6$ and have been observed to be a part of their solution speciation.^{35,36} The hexanitrate moiety is less frequently observed in trivalent metals, reported here for trivalent $5f$ -ions for the first time.^{37–39} The hexanitrate moiety is not likely a component of trivalent f -ion solution speciation owing to the weakly coordinating nature of nitrate and the large hydration enthalpies of these ions.⁴⁰ Nevertheless, this report and those prior, indicate that the trivalent metal hexanitrate moiety may be incorporated into hybrid perovskite phases across the entire periodic table.

To assess the An-nitrate ligand interactions, relativistic density functional theory (DFT) calculations were performed on $[\text{An}(\text{NO}_3)_6\text{K}_6]^{3+}$ clusters cut out from the crystal structures and optimized in the gas phase. Similar calculations were also performed on the isoelectronic $4f$ homologues Eu(III) and Gd(III) to assess differences between the lanthanide and actinide metal-ligand interactions in these systems. The relaxed M-O bond distances agree within 0.02 Å with the crystal ones (See Tables 3 and 2). The Cm-O distances are 0.006 Å shorter than the Am-O ones, as expected from the contraction of the ionic radii along the actinide series⁴¹. The topology of the An–ONO₂ bonds probed by the Quantum Theory of Atoms-in-Molecules (QTAIM) can be probed by several descriptors determined at the bond critical point, namely the value of the density (ρ_b), the Laplacian ($\nabla^2\rho_b$) and the ratio between the absolute potential energy density and the kinetic energy density $|V_b|/G_b$. Finally the delocalization index DI is a measure of the bond order. The ρ_b values are smaller than 0.1 and the Laplacians of the density are all positive, suggesting closed-shell interactions according to the standard QTAIM classification.^{42,43} However, the $|V_b|/G_b$ ratio larger than 1 suggest some covalency in the bond, which slightly decreases from Am to Cm, indicating that bonds are somewhat more ionic in the Cm complex than in the Am one consistent with periodic trends observed for gas phase Am and Cm nitrate complexes.¹⁸ The analysis of the Eu and Gd lanthanide homologue complexes show that in comparison to the Am and Cm complexes, the lanthanide nitrate interactions are more ionic than those observed in the actinides.

Table 3 Average M-O bond distances in (Å) from QM calculations on the $[\text{M}(\text{NO}_3)_6\text{K}_6]^{3+}$ chemical model. QTAIM parameters at the M-O bond critical points (density ρ_b , Laplacian $\nabla^2\rho_b$ and ratio $|V_b|/|G_b|$ between the the potential energy density and the kinetic energy density, and the delocalization index)

Property	Eu	Gd	Am	Cm
$r(\text{M-O})$	2.584	2.589	2.625	2.618
ρ_b	0.035	0.035	0.037	0.037
$\nabla^2\rho_b$	0.132	0.126	0.138	0.137
$ V_b / G_b $	1.015	1.017	1.053	1.041
DI(An-O)	0.251	0.240	0.281	0.265

Raman spectra were collected on the single crystals of the Am and Cm phases. These spectra, Figure S3 in the ESI† are dominated by the vibrational modes of the NO_3^- and $(\text{CH}_3)_4\text{N}^+$ ions.^{44,45} The most intense feature is associated with the symmetric stretching of the NO_3^- at 1054(1) cm^{-1} in both spectra. This assignment is confirmed by the Raman spectra computed for the $[\text{Cm}(\text{NO}_3)_6\text{K}_6]^{3+}$ cluster model shown in Figure S4 of the ESI†, where this symmetric stretching mode appears at 1154 cm^{-1} . The symmetric and asymmetric frequencies associated with the tetramethylammonium cations are observed at 755 and 952 cm^{-1} respectively. The asymmetric mode of the $(\text{CH}_3)_4\text{N}^+$ is triply degenerate and only one peak is observed in the Raman spectrum here providing confidence to the symmetry of the space group assigned. The additional bands in the multiplet of peaks between 700–760 cm^{-1} involve contributions from the nitrate ion bending modes in addition to the C-N stretches from the quarternary amine. Indeed bending vibrations come out at 780 cm^{-1} in the cluster model, while that at 730 cm^{-1} correspond to nitrate rocking modes (cf. Figure S4 of the ESI†). Lower frequency peaks observed around 365 cm^{-1} and 455 cm^{-1} are attributable to the NCH_4 deformation modes. A tentative and cautioned assignment of the Am or $\text{Cm}(\text{O}_2\text{NO})_6$ vibration is made based off of prior observations of Raman bands in U, Np, and Pu data and are assigned to the shoulders near 204 and 211 cm^{-1} respectively.¹⁶ These features are obscured by the intense lattice modes associated with the K^+ ions at these lower frequencies but consistent with the frequencies observed more clearly in other actinide nitrates and near those frequencies attributed to An–NCS vibrations previously.¹⁷

In summary, the synthesis, structure and electronic properties of twelve coordinate homoleptic hexanitrate complexes of the transuranium ions americium and curium have been reported. The synthesized complexes take on a hybrid double perovskite structure in $Fm\bar{3}m$ expanding the synthetic phase space of the hybrid double perovskites into the transuranium elements. The high-symmetry of these f -ion compounds, and their centrosymmetric symmetry, makes them especially useful materials for the comparative study of lanthanide and actinide electronic structure and our understanding of the role of f -element metal-ligand bonding in chemical separations.

Author Contributions

MLT, SS, and REW collected and analysed the experimental data. VV performed and analysed the computational data. VV and REW wrote the manuscript.

Conflicts of interest

There are no conflicts to declare.

Notes and references

- M. J. Polinski, S. Wang, E. V. Alekseev, W. Depmeier, G. Liu, R. G. Haire and T. E. Albrecht-Schmitt, *Angew. Chem.*, 2012, **124**, 1905–1908.
- S. K. Cary, M. Vasiliu, R. E. Baumbach, J. T. Stritzinger, T. D. Green, K. Diefenbach, J. N. Cross, K. L. Knappenberger, G. Liu, M. A. Silver *et al.*, *Nat. Commun.*, 2015, **6**, 1–8.
- K. P. Carter, K. M. Shield, K. F. Smith, Z. R. Jones, J. N. Wacker, L. Arnedo-

- Sanchez, T. M. Mattox, L. M. Moreau, K. E. Knope, S. A. Kozimor *et al.*, *Nature*, 2021, **590**, 85–88.
- 4 M. G. Ferrier, E. R. Batista, J. M. Berg, E. R. Birnbaum, J. N. Cross, J. W. Engle, H. S. La Pierre, S. A. Kozimor, J. S. Lezama Pacheco, B. W. Stein *et al.*, *Nat. Commun.*, 2016, **7**, 1–8.
 - 5 J. Su, E. R. Batista, K. S. Boland, S. E. Bone, J. A. Bradley, S. K. Cary, D. L. Clark, S. D. Conradson, A. S. Ditter, N. Kaltsoyannis *et al.*, *J. Am. Chem. Soc.*, 2018, **140**, 17977–17984.
 - 6 S. G. Minasian, J. M. Keith, E. R. Batista, K. S. Boland, D. L. Clark, S. D. Conradson, S. A. Kozimor, R. L. Martin, D. E. Schwarz, D. K. Shuh *et al.*, *J. Am. Chem. Soc.*, 2012, **134**, 5586–5597.
 - 7 I. D. Prodan, G. E. Scuseria and R. L. Martin, *Phys. Rev. B*, 2007, **76**, 033101.
 - 8 R. Diamond, K. Street Jr and G. T. Seaborg, *J. Am. Chem. Soc.*, 1954, **76**, 1461–1469.
 - 9 M. P. Jensen and A. H. Bond, *J. Am. Chem. Soc.*, 2002, **124**, 9870–9877.
 - 10 S. K. Cary, J. Su, S. S. Galley, T. E. Albrecht-Schmitt, E. R. Batista, M. G. Ferrier, S. A. Kozimor, V. Mocko, B. L. Scott, C. E. Van Alstine *et al.*, *Dalton Trans.*, 2018, **47**, 14452–14461.
 - 11 M. A. Silver, S. K. Cary, J. A. Johnson, R. E. Baumbach, A. A. Arico, M. Luckey, M. Urban, J. C. Wang, M. J. Polinski, A. Chemey *et al.*, *Science*, 2016, **353**, aaf3762.
 - 12 R. E. Wilson, *Inorg. Chem.*, 2011, **50**, 5663–5670.
 - 13 D. D. Schnaars and R. E. Wilson, *Inorg. Chem.*, 2012, **51**, 9481–9490.
 - 14 M. Autillo and R. E. Wilson, *European Journal of Inorganic Chemistry*, 2017, **2017**, 4834–4839.
 - 15 R. E. Wilson, *Inorg. Chem.*, 2015, **54**, 10208–10213.
 - 16 M. Autillo and R. E. Wilson, *Inorg. Chem.*, 2019, **58**, 3203–3210.
 - 17 R. E. Wilson, T. J. Carter, M. Autillo and S. Stegman, *Chem. Commun.*, 2020, **56**, 2622–2625.
 - 18 A. Kovács, P. D. Dau, J. Marçalo and J. K. Gibson, *Inorganic Chemistry*, 2018, **57**, 9453–9467.
 - 19 P. D. Dau, M. Vasiliu, K. A. Peterson, D. A. Dixon and J. K. Gibson, *Chemistry–A European Journal*, 2017, **23**, 17369–17378.
 - 20 L. Morss and J. Fuger, *Inorg. Chem.*, 1969, **8**, 1433–1439.
 - 21 L. R. Morss, M. Siegal, L. Stenger and N. Edelstein, *Inorg. Chem.*, 1970, **9**, 1771–1775.
 - 22 K. Bagnall, J. Laidler and M. Stewart, *J. Chem. Soc. A*, 1968, 133–136.
 - 23 A. S. R. Chesman, D. R. Turner, G. B. Deacon and S. R. Batten, *Acta Crystallogr., Sect. E: Struct. Rep. Online*, 2006, **62**, m1942 – m1943.
 - 24 A. S. R. Chesman, D. R. Turner, G. B. Deacon and S. R. Batten, *J. Coord. Chem.*, 2007, **60**, 2191–2196.
 - 25 J. K. Nimmo and B. W. Lucas, *Acta Cryst.*, 1976, **B32**, 1968–1971.
 - 26 Z. Deng, F. Wei, F. Brivio, Y. Wu, S. Sun, P. D. Bristowe and A. K. Cheetham, *J. Phys. Chem. Lett.*, 2017, **8**, 5015–5020.
 - 27 K. M. Murdoch, R. Cavellec, E. Simoni, M. Karbowiak, S. Hubert, M. Illemassene and N. M. Edelstein, *J. Chem. Phys.*, 1998, **108**, 6353–6361.
 - 28 M. V. Hoehn and D. G. Karraker, *J. Chem. Phys.*, 1974, **60**, 393–397.
 - 29 G. Kieslich, S. Sun and A. K. Cheetham, *Chem. Sci.*, 2015, **6**, 3430–3433.
 - 30 G. Kieslich, S. Sun and A. K. Cheetham, *Chem. Sci.*, 2014, **5**, 4712–4715.
 - 31 Y. Wu, S. Shaker, F. Brivio, R. Murugavel, P. D. Bristowe and A. K. Cheetham, *J. Am. Chem. Soc.*, 2017, **139**, 16999–17002.
 - 32 C. Shi, L. Ye, Z.-X. Gong, J.-J. Ma, Q.-W. Wang, J.-Y. Jiang, M.-M. Hua, C.-F. Wang, H. Yu, Y. Zhang and H.-Y. Ye, *J. Am. Chem. Soc.*, 2020, **142**, 545–551.
 - 33 C. Shi, J.-J. Ma, J.-Y. Jiang, M.-M. Hua, Q. Xu, H. Yu, Y. Zhang and H.-Y. Ye, *J. Am. Chem. Soc.*, 2020, **142**, 9634–9641.
 - 34 Q. Xu, L. Ye, R.-M. Liao, Z. An, C.-F. Wang, L.-P. Miao, C. Shi, H.-Y. Ye and Y. Zhang, *Chem. Eur. J.*, 2022, **28**, e202103913.
 - 35 T. A. Beineke and J. Delgaudio, *Inorg. Chem.*, 1968, **7**, 715–721.
 - 36 P. G. Allen, D. K. Veirs, S. D. Conradson, C. A. Smith and S. F. Marsh, *Inorg. Chem.*, 1996, **35**, 2841–2845.
 - 37 A. Zalkin, J. D. Forrester and D. H. Templeton, *The Journal of Chemical Physics*, 1963, **39**, 2881–2891.
 - 38 M. S. Wickleder, *Chemical Reviews*, 2002, **102**, 2011–2088.
 - 39 C. Addison and D. Sutton, *Progress in Inorganic Chemistry*, 1967, 195–286.
 - 40 C. Bonal, J.-P. Morel and N. Morel-Desrosiers, *J. Chem. Soc., Faraday Trans.*, 1998, **94**, 1431–1436.
 - 41 R. D. Shannon, *Acta Crystallogr. A*, 1976, **32**, 751–767.
 - 42 E. Espinosa, I. Alkorta, J. Elguero and E. Molins, *J. Chem. Phys.*, 2002, **117**, 5529–5542.
 - 43 C. Lepetit, P. Fau, K. Fajerweg, M. L. Kahn and B. Silvi, *Coord. Chem. Rev.*, 2017, **345**, 150–181.
 - 44 G. Kabisch and M. Klose, *J. Raman Spectrosc.*, 1978, **7**, 311–315.
 - 45 C. C. Addison, D. W. Amos, D. Sutton and W. H. H. Hoyle, *J. Chem. Soc. A*, 1967, 808–812.